iScience

CellPress
OPEN ACCESS

Article

# NRBF2 regulates the chemoresistance of small cell lung cancer by interacting with the P62 protein in the autophagy process

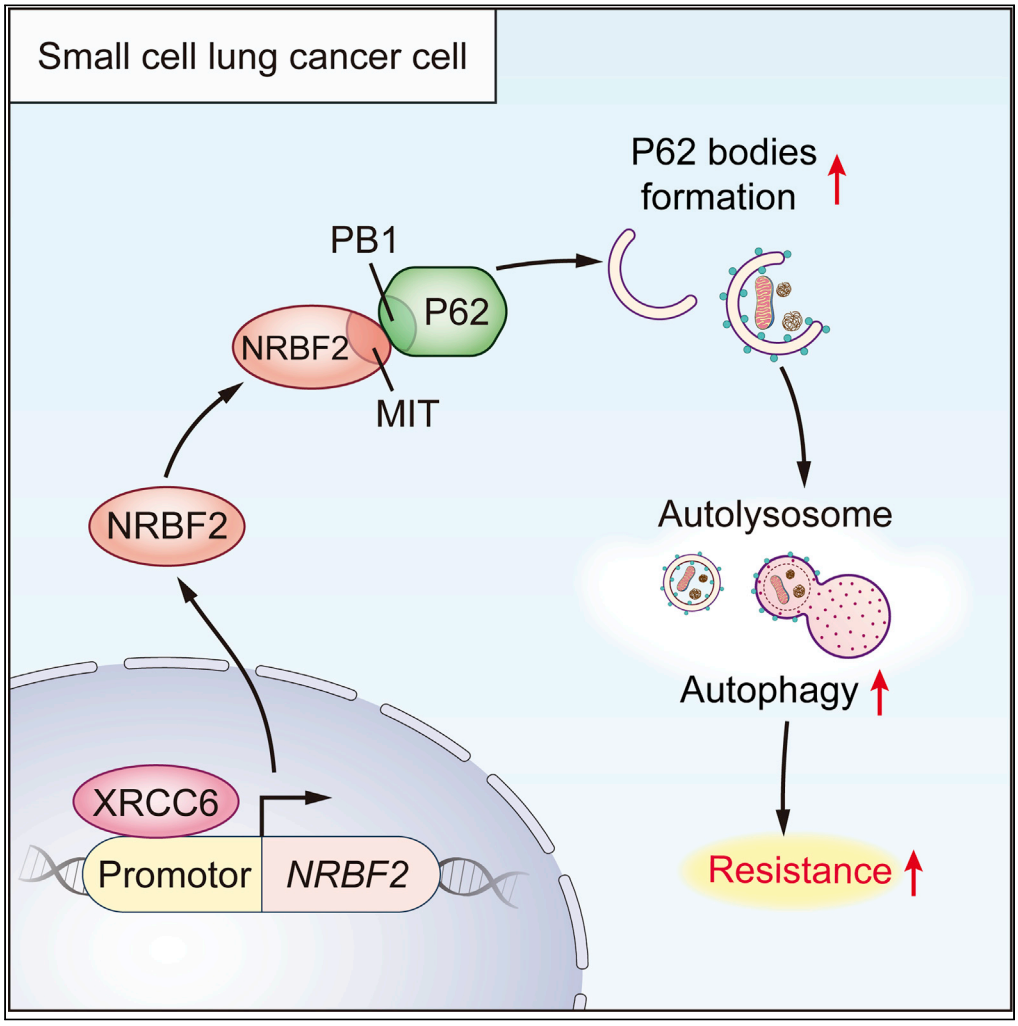


Weitao Shen, Peng Luo, Yueqin Sun, ..., Jian Zhang, Hai-Hong Wang, Ting Wei

zhangjian@i.smu.edu.cn (J.Z.)
haihwang@163.com (H.-H.W.)
weitingyouyou@qq.com (T.W.)

## Highlights

NRBF2 promoted the chemoresistance of SCLC *in vitro* and *in vivo*

The chemoresistance induced by NRBF2 was mediated via autophagy in SCLC

NRBF2 interacting with P62 contributed to autophagic P62 bodies' formation

NRBF2 was regulated by XRCC6 via direct binding to the NRBF2 gene promoter

Shen et al., iScience 25, 104471
June 17, 2022 © 2022
https://doi.org/10.1016/j.isci.2022.104471

iScience

CellPress
OPEN ACCESS

Article

# NRBF2 regulates the chemoresistance of small cell lung cancer by interacting with the P62 protein in the autophagy process

Weitao Shen,[1,7] Peng Luo,[1,7] Yueqin Sun,[1,7] Wei Zhang,[1,7] Ningning Zhou,[2,7] Hongrui Zhan,[3] Qingxi Zhang,[4] Jie Shen,[1] Anqi Lin,[1] Quan Cheng,[5] Qiongyao Wang,[1] Jian Zhang,[1,*] Hai-Hong Wang,[6,*] and Ting Wei[1,8,*]

## SUMMARY

**Reversing chemotherapy resistance in small cell lung cancer (SCLC) is crucial to improve patient prognosis. The present study aims to investigate the underlying mechanisms in SCLC chemoresistance. We see that nuclear receptor binding factor 2 (NRBF2) is a poor prognostic factor in SCLC. The effects of NRBF2 on chemoresistance were determined in SCLC. The underlying molecular mechanisms of NRBF2 in the autophagy process in SCLC were examined. NRBF2 positively regulated autophagy, leading to drug resistance in SCLC. The MIT domain of NRBF2 directly interacted with the PB1 domain of P62. This interaction increased autophagic P62 body formation, revealing the regulatory role of NRBF2 in autophagy. Notably, NRBF2 was directly modulated by the transcription factor XRCC6. The MIT domain of NRBF2 interacts with the PB1 domain of P62 to regulate the autophagy process, resulting in SCLC chemoresistance. NRBF2 is likely a useful chemotherapy response marker and therapeutic target in SCLC.**

## INTRODUCTION

Lung cancer has the highest morbidity and mortality rates globally, and the number of deaths caused by lung cancer exceeds 1 million every year worldwide (Siegel et al., 2017). Small cell lung cancer (SCLC) accounts for approximately 15% of lung cancers (Sabari et al., 2017). In addition, SCLC is the most aggressive subtype of lung cancer. The average 2-year survival rate of patients with SCLC is less than 5%, and 90% of patients die within 5 years of diagnosis. Approximately 90% of SCLC patients have tissue invasion, lymphatic tract involvement or distant metastasis at diagnosis (Hamilton et al., 2016; Rudin and Poirier, 2017). Chemotherapy is a critical treatment option for SCLC. Although the initial remission rate of chemotherapy is high in SCLC, drug resistance rapidly develops and causes tumor relapse (Lawson et al., 2011). Therefore, it is crucial to elucidate the mechanisms of chemoresistance and determine therapeutic targets for SCLC.

Several studies have shown that the cellular autophagy process is involved in the protective mechanism of tumors, leading to increased drug resistance in cancer chemotherapy (Kim et al., 2017; Sun et al., 2011). Autophagy is a cellular survival response to external stressors, in which cells encapsulate their dysfunctional proteins and organelles to form vesicles that degrade in the lysosome (Jacob et al., 2017; Shen et al., 2017). It includes five stages: induction, nucleation, elongation, autophagosome formation, and digestion in autolysosomes. Autophagy is a potential mechanism of drug resistance in tumors (Li et al., 2017; Zhang et al., 2015). We previously reported that autophagy protects SCLC cells from the cytotoxic effects of chemotherapeutic drugs (Wang et al., 2018). However, the key molecules or detailed mechanisms associated with chemoresistance in the autophagy regulation process remain to be elucidated. Autophagy inhibition combined with chemotherapy is a promising strategy for cancer treatment, and this strategy has become a major focus of cancer research (Janku et al., 2011; Rubinsztein et al., 2012; Shen et al., 2020). Thus, the search for chemoresistance-related autophagy genes can provide new targets to solve the problem of drug resistance in SCLC treatment.

To identify potential genes that function in SCLC chemoresistance, nuclear receptor binding factor 2 (NRBF2) was identified by RNA sequencing in local samples from SCLC patients in this study. Next, we investigated the biological function of NRBF2 in the chemotherapy response both *in vivo* and *in vitro*.

[1]Department of Oncology, Zhujiang Hospital, Southern Medical University, 253 Industrial Avenue, Guangzhou 510282, Guangdong, People's Republic of China

[2]Department of Medical Oncology, Sun Yat-Sen University Cancer Center, State Key Laboratory of Oncology in South China, Collaborative Innovation Center for Cancer Medicine, Guangzhou 510282, Guangdong, People's Republic of China

[3]Department of Rehabilitation, The Fifth Affiliated Hospital of Sun Yat-sen University, Zhuhai 519000, Guangdong, People's Republic of China

[4]The Second School of Clinical Medicine, Southern Medical University, Guangzhou 510515, Guangdong, People's Republic of China

[5]Department of Neurosurgery, Xiangya Hospital, Central South University, Changsha 410008, Hunan, People's Republic of China

[6]Department of Histology and Embryology, School of Basic Medical Sciences, Southern Medical University, Guangzhou 510515, Guangdong, People's Republic of China

[7]These authors contributed equally

[8]Lead contact

*Correspondence: zhangjian@i.smu.edu.cn (J.Z.), haihwang@163.com (H.-H.W.), weitingyouyou@qq.com (T.W.)

https://doi.org/10.1016/j.isci.2022.104471

Furthermore, a close association between autophagy and NRBF2 was determined in SCLC, and we found that NRBF2 promoted chemotherapy resistance in SCLC by regulating autophagy. To clarify how NRBF2 affects autophagy in SCLC chemoresistance, we assessed the interaction of NRBF2 with other molecules and searched for its potential upstream regulator. Using mass spectrometry (MS), we found that the NRBF2 MIT domain was responsible for the interaction with autophagy core protein sequestosome 1/P62 (hereafter referred to as P62) through the N-terminal Phox and Bem1 (PB1) domain of P62. With the cooperation of this interaction, ubiquitin-positive and P62-positive protein bodies (named P62 bodies) formed and recruited target cargoes to the autophagosome. The consequences of these interactions revealed that NRBF2 interacted with the P62 protein to enhance autophagy by activating P62 body formation, resulting in chemotherapy resistance. In addition, the regulator of NRBF2 was identified as the transcription factor XRCC6, which is directly bound to the NRBF2 gene promoter. Overall, this study identifies a therapeutic target or potential biomarker to predict SCLC chemoresistance.

## RESULTS

### NRBF2 is upregulated in chemoresistant SCLC clinical tissues and cells

The impact of gene expression on the prognosis of patients is shown in the volcano map (Figure 1A). Among the top 20 genes with the most significant differences mentioned before, we found that DNAJA3, CTRL, UFC1, and NRBF2 might be autophagy-related genes by searching the GeneCard database and published literature. To determine chemoresistance-related autophagy genes, the expression of DNAJA3, CTRL, UFC1, and NRBF2 was examined in two pairs of chemosensitive and chemoresistant SCLC cell lines, H69/H69AR and H446/H446DDP. NRBF2 was highly expressed in both chemoresistant SCLC cell lines (Figure 1B). Univariate and multivariable Cox regression models were used to explore the impact of NRBF2 expression on the survival of SCLC patients. After excluding the influence of common clinical factors, high expression of NRBF2 was an independent prognostic factor for the worse survival of SCLC patients (Figure 1C). Kaplan-Meier analysis of the local SCLC cohort to evaluate the impact of NRBF2 expression on the survival of SCLC patients revealed a correlation between high NRBF2 expression and poor overall survival (Figure 1D). In addition, we explored the association with NRBF2 expression and key lineage oncogenes including ASCL1, NEUROD1, SLFN11, Myc, and POU2F3 (Figure S1). The expression of ASCL1, NEUROD1, POU2F3, Myc, and SLFN11 was evaluated in chemosensitive and chemoresistant SCLC cells (Figure S2). Results showed that the expression of SLFN11 and c-Myc was highly expressed in chemoresistant SCLC cells. Besides, the disease free survival (DFS) rate for SCLC patients with different expressions of ASCL1, NEUROD1, and SLFN11 are shown in Figure S3, revealing a significant correlation between high ASCL1 expression and poor DFS rate.

To further determine the clinical significance of NRBF2 in predicting and reversing chemoresistance in SCLC, the NRBF2 level in samples from SCLC patients was analyzed by immunohistochemistry (IHC). The expression level of NRBF2 was significantly higher in samples from chemoresistant patients than in samples from drug-sensitive patients (Figure 1E).

Subsequently, we used H69/H69AR and H446/H446DDP cells to further explore the role of NRBF2 in SCLC chemoresistance. Notably, both western blotting and immunofluorescence revealed that NRBF2 expression was significantly increased in chemoresistant SCLC cells compared with that in chemosensitive cells (Figures 1F–1H). Interestingly, NRBF2 protein was predominantly expressed in the cytoplasm according to the immunofluorescence analysis. These results suggested that NRBF2 might be related to SCLC chemoresistance.

### NRBF2 promotes the chemoresistance of SCLC *in vitro*

To explore the effect of NRBF2 on SCLC chemoresistance, we developed chemosensitive SCLC cells (H69 and H446) with stable overexpression of NRBF2 and chemoresistant SCLC cells (H69AR and H446DDP) with stable downregulation of NRBF2 for further study (Figures S4A and S4B). Next, we examined the sensitivity of SCLC cells to chemotherapeutic drugs (cisplatin, CDDP; etoposide, and VP16) using Cell Counting Kit-8 (CCK-8) assays. The half-maximal inhibitory concentration (IC50) was increased after overexpressing NRBF2, whereas the downregulation of NRBF2 markedly decreased the IC50 values in SCLC cells (Figures 2A–2D, S5, and S6). Because many chemotherapeutic drugs exhibit antitumor effects partially by inducing cell apoptosis, we determined whether apoptosis was regulated by NRBF2 in SCLC cells. Apoptosis induction was evaluated using cleaved caspase 3 immunofluorescence assays and terminal deoxynucleotidyl transferase (TdT) dUTP nick end labeling (TUNEL) assays. The induction of apoptosis was

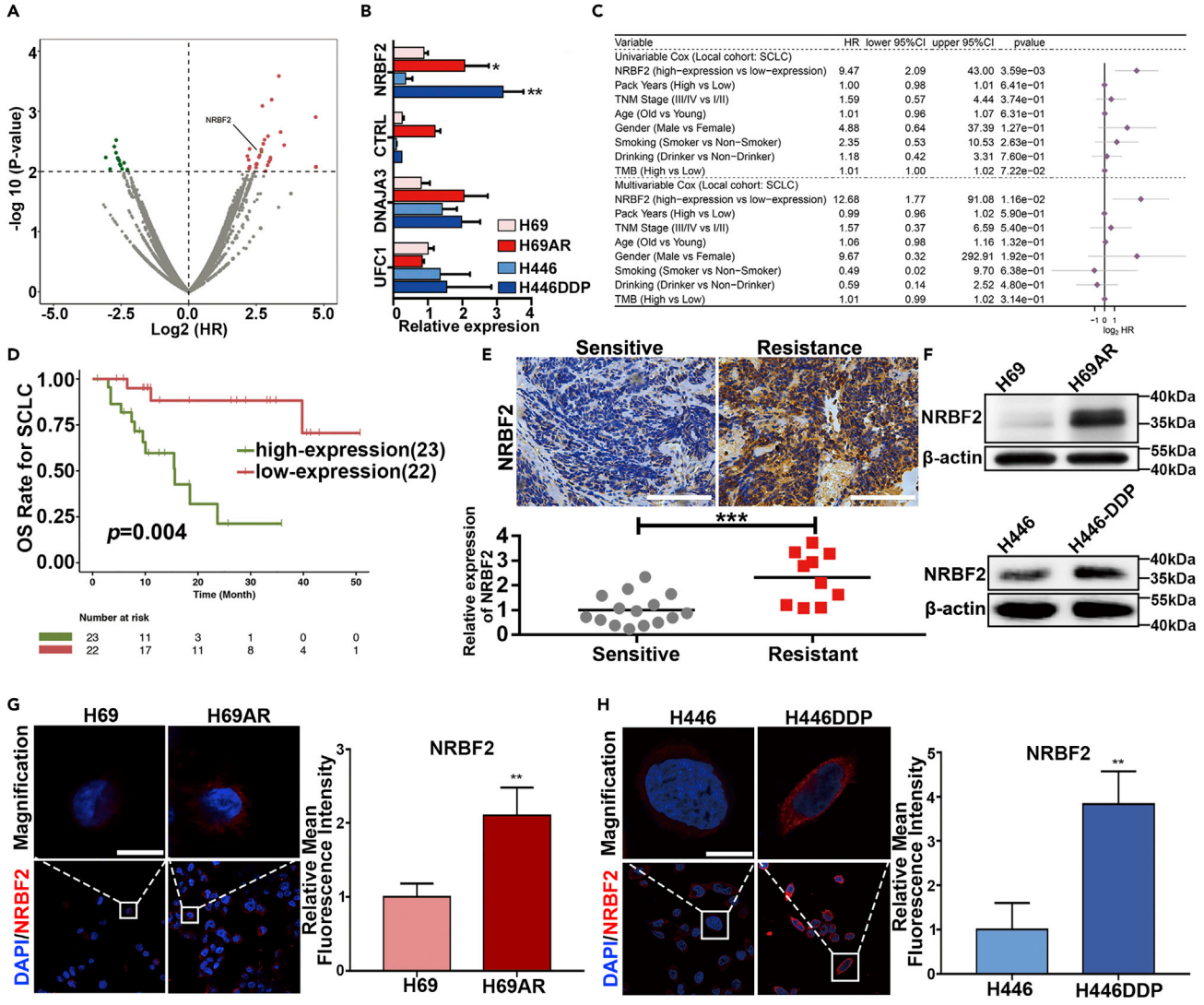


**Figure 1. Expression of NRBF2 and the clinical significance of NRBF2 in SCLC**

(A) Volcano plot of the effect of NRBF2 expression on the survival of SCLC patients.

(B) qRT-PCR analysis of DNAJA3, CTRL, UFC1, and NRBF2 in two pairs of chemosensitive and chemoresistant SCLC cells. The data are presented as means ± SD of three independent experiments. **p < 0.01; ***p < 0.001.

(C) Univariate and multivariate Cox regression models were used to explore the impact of NRBF2 expression on the survival of SCLC patients.

(D) Overall survival (OS) rate for SCLC patients with low NRBF2 expression (n = 22) and high NRBF2 expression (n = 23). Statistical significance was determined by the log-rank test. p = 0.004.

(E) Representative IHC staining of NRBF2 in samples from chemosensitive and chemoresistant SCLC tissues. Relative expression of NRBF2 in samples of 15 chemosensitive and 10 chemoresistant SCLC tissues. ***, p < 0.001. Scale bars, 100 μm.

(F) Western blot analysis of NRBF2 expression in two pairs of chemosensitive and chemoresistant SCLC cells, H69/H69AR and H446/H446DDP.

(G and H) Immunofluorescence analysis of NRBF2 in H69/H69AR and H446/H446DDP cells. Scale bars, 50 μm. Quantification of NRBF2 expression detected by immunofluorescence is shown. The data originated from 3 independent experiments. **, p < 0.01.

attenuated in SCLC cells overexpressing NRBF2 and was activated after NRBF2 knockdown (Figures 2E, 2F, S7A, and S7B). Similarly, the significant effect of altering NRBF2 levels on SCLC cells was identified by flow cytometry (Figure S8). In subsequent experiments, western blot assays also demonstrated that the expression of the apoptosis-related cleaved PARP protein was significantly reduced in SCLC cells overexpressing NRBF2 (Figure 2G). By contrast, NRBF2 knockdown dramatically increased the expression of cleaved PARP in chemoresistant SCLC cells (Figure 2H). Together, these results indicated that NRBF2 expression enhanced the chemoresistance of SCLC cells *in vitro*.

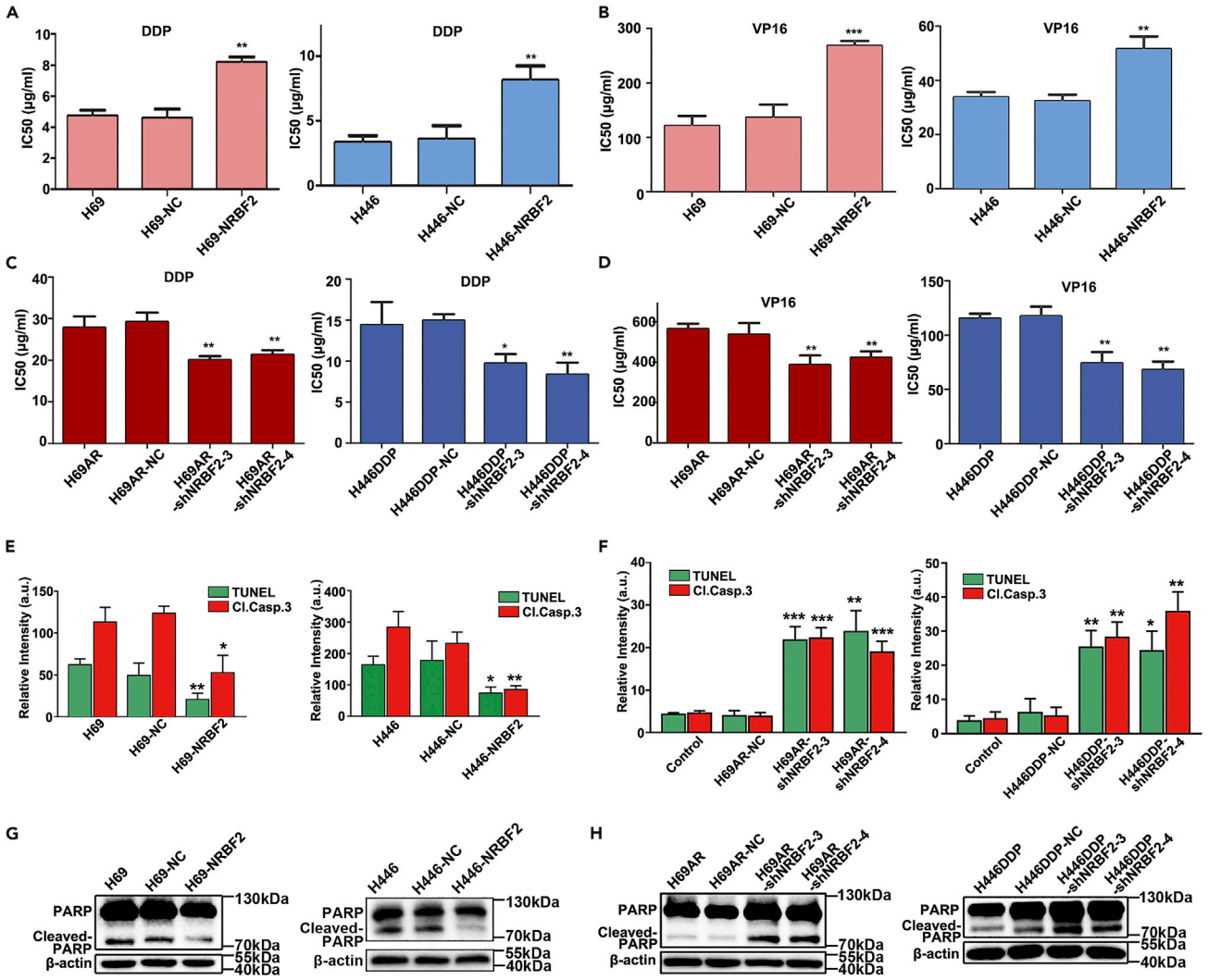


**Figure 2. NRBF2 induces the chemoresistance of SCLC cells *in vitro***

(A and B) CCK-8 assays showed that NRBF2 overexpression increased the IC50 values of chemotherapeutic agents of chemosensitive H69 and H446 cells.

(C and D) CCK-8 assays showed that downregulation of NRBF2 decreased the IC50 values of chemoresistant H69AR and H446DDP cells.

(E) Cell apoptosis induced by chemotherapeutic agents was examined by cleaved caspase 3 and TUNEL staining after overexpressing NRBF2 in H69 and H446 cells. The data are presented as means ± SD of three independent experiments. *$p < 0.05$; **$p < 0.01$.

(F) Cell apoptosis induced by chemotherapeutic agents was examined by cleaved caspase 3 and TUNEL staining after the downregulation of NRBF2 in H69AR and H446DDP cells. The data were presented as means ± SD of three independent experiments. *$p < 0.05$; **$p < 0.01$.

(G and H) Western blotting was applied to examine the apoptosis of NRBF2-overexpressing or NRBF2-downregulated SCLC cells.

## NRBF2 induces chemoresistance in SCLC *in vivo*

To examine the effect of NRBF2 on the chemoresistance of SCLC *in vivo*, we established a subcutaneous transplantation tumor model in nude mice using SCLC cells with NRBF2 overexpression or knockdown. Tumor-bearing mice were divided into four groups, and each group was intraperitoneally administered saline or chemotherapeutic drugs (CDDP and VP-16). When nude mice were treated with chemotherapeutic drugs, the subcutaneous xenograft tumors derived from cells with NRBF2 knockdown exhibited more remarkable growth inhibition than the tumors derived from control cells (Figures 3A–3C). Then, we performed a tumorigenesis assay by subcutaneously injecting NRBF2 overexpressing cells or negative control cells into nude mice. After treatment with chemotherapeutic drugs, tumors derived from NRBF2-overexpressing cells grew more rapidly than those derived from negative control cells (Figures 3D–3F). Interestingly, tumors with NRBF2 knockdown grew more slowly than tumors derived from control cells, and tumor growth was accelerated by NRBF2 overexpressing under intraperitoneally injection with saline. It

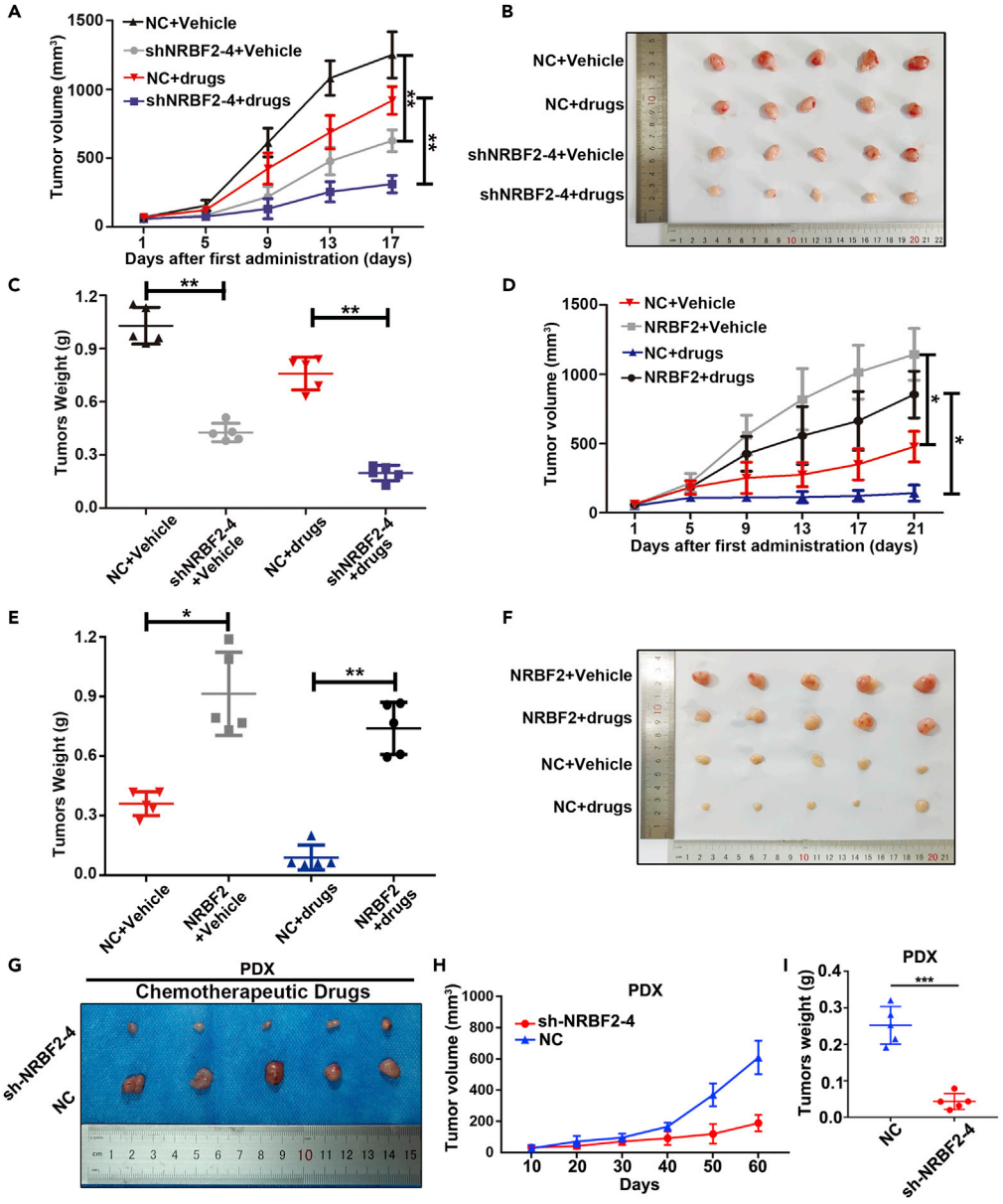


**Figure 3. Effects of NRBF2 on SCLC chemoresistance *in vivo***

(A) Tumor growth of NRBF2 knockdown groups was measured. H69AR cells were stably transfected with shNC or shNRBF2-4. Each group of cells was injected into mice, and chemotherapeutic agents (etoposide and cisplatin) or vehicles were injected intraperitoneally. **$p < 0.01$.

(B and C) Effect of NRBF2 on resistance to chemotherapeutic agents (etoposide and cisplatin) in nude mice and measurement of the tumor weights of different groups. **$p < 0.01$.

(D) Tumor growth of NRBF2 overexpression groups was measured. H69 cells stably overexpressing NRBF2 or control cells were injected into mice, and chemotherapeutic agents (etoposide and cisplatin) or vehicles were injected intraperitoneally. *$p < 0.05$.

(E and F) Effect of NRBF2 on sensitivity to chemotherapeutic agents (etoposide and cisplatin) in nude mice and measurement of the tumor weights of different groups. *$p < 0.05$, **$p < 0.01$.

(G) Image of tumors derived from mice on day 60 after re-engraftment of PDX-resistant tumor tissue. The mice were treated with chemotherapeutic agents (etoposide and cisplatin).

(H) Growth curve of the tumor volumes in each indicated group of PDX models.

(I) Tumor weights of tumors harboring NRBF2-downregulating cells or empty vector-infected cells.

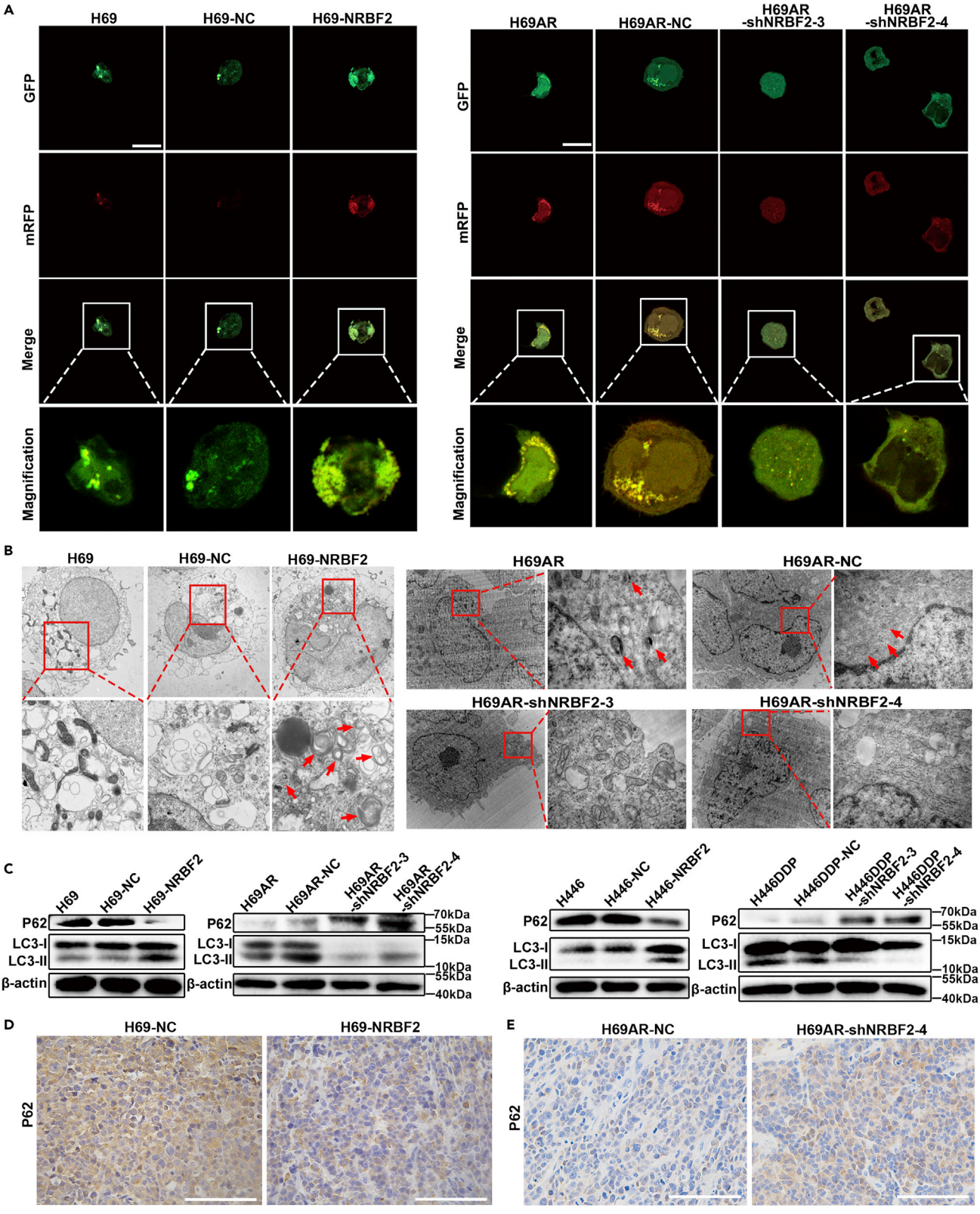
A
H69
H69-NC
H69-NRBF2
H69AR
H69AR-NC
H69AR -shNRBF2-3
H69AR -shNRBF2-4
GFP
mRFP
Merge
Magnification
B
H69
H69-NC
H69-NRBF2
H69AR
H69AR-NC
H69AR-shNRBF2-3
H69AR-shNRBF2-4
C
H69
H69-NC
H69-NRBF2
H69AR
H69AR-NC
H69AR -shNRBF2-3
H69AR -shNRBF2-4
P62
LC3-I
LC3-II
β-actin
70kDa
55kDa
15kDa
10kDa
55kDa
40kDa
H446
H446-NC
H446-NRBF2
H446DDP
H446DDP-NC
H446DDP -shNRBF2-3
H446DDP -shNRBF2-4
D
H69-NC
H69-NRBF2
P62
E
H69AR-NC
H69AR-shNRBF2-4
P62

**Figure 4. NRBF2 promotes autophagy in SCLC cells**

(A) Laser confocal microscopy analysis of LC3 puncta in SCLC cells transiently expressing the mRFP-GFP-LC3 fusion protein. Scale bars, 20 μm.

(B) Autophagosomes were examined by TEM to validate the effect of NRBF2 on autophagy in SCLC cells. The magnified view of the electron photomicrograph shows autophagosomes. Arrows, autophagosomes.

(C) Western blot analysis of the autophagy markers LC3 and P62 in SCLC cells with NRBF2 overexpression or knockdown.

(D and E) Representative IHC staining of autophagy-associated protein P62 in subcutaneous xenografts with NRBF2 overexpression or downregulation. Scale bars, 100 μm.

suggested that NRBF2 might promote growth to some extent. In addition, NRBF2 expression in the tumor xenografts was identified by IHC (Figures S9A and S9B). These data indicated that NRBF2 induced SCLC chemoresistance.

Next, to further identify the effects of NRBF2 on SCLC chemoresistance, we used a patient-derived xenograft (PDX) model with tumor tissues from SCLC patients. Xenograft tumor tissues from fresh drug-resistant PDX xenograft tumors were digested into single-cell suspensions. One cell line was established and stably downregulated the expression of NRBF2 (Figure S10). Next, we injected an equal number of cells into severely immunodeficient NCG mice subcutaneously. The results similarly showed that the chemosensitivity of mice bearing a tumor comprising NRBF2-downregulating cells was significantly higher than that of mice bearing the corresponding control tumor comprising empty vector-infected cells (Figures 3G–3I).

These findings indicated that NRBF2 affected the chemosensitivity of SCLC *in vivo*, further confirming the effectiveness of NRBF2 as a therapeutic target or prognostic biomarker for SCLC chemoresistance.

## NRBF2 regulates autophagy in SCLC cells

To understand the mechanism by which NRBF2 induces SCLC chemoresistance, we examined whether NRBF2 affects the key survival program of SCLC cells, the autophagy process. We employed chemoresistant SCLC cells with NRBF2 downregulation and chemosensitive SCLC cells with NRBF2 overexpression. The mRFP-GFP-LC3 adenovirus translocation assay indicated an increase in autophagy concurrent with NRBF2 overexpression, whereas autophagy was attenuated after NRBF2 knockdown (Figures 4A, S11A, and S11B). Transmission electron microscopy (TEM) analysis showed that the number of autophagic vesicles was significantly decreased after NRBF2 knockdown, whereas the number of autophagic vesicles was increased in NRBF2-overexpressing cells compared with that in control cells (Figure 4B).

Next, we applied western blotting to examine the protein expression levels of LC3 and P62, two markers of autophagy. Knockdown of the NRBF2 gene inhibited autophagy in drug-resistant H69AR and H446DDP cells, whereas NRBF2 overexpression remarkably induced autophagy in drug-sensitive H69 and H446 cells (Figure 4C). Furthermore, we examined the expression of the autophagy marker P62 in the aforementioned SCLC subcutaneous tumor models using IHC. P62 expression was directly correlated with NRBF2 (Figures 4D and 4E). In addition, we explored the relationship of SLFN11 expression to autophagy and the NRBF2. The regulation of SLFN11 could not significantly affect autophagy and the NRBF2 expression in SCLC cells (Figure S12).

Therefore, NRBF2 affected autophagy in SCLC.

## NRBF2-induced chemoresistance is mediated by autophagy in SCLC

Autophagy plays an important role in the survival of tumor cells exposed to chemotherapeutic drugs. To further understand the relationship between NRBF2-induced chemoresistance and autophagy, we used chloroquine (CQ), an autophagy inhibitor that blocks autophagic cargo degradation in lysosomes. The drug sensitivity of H69 and H446 cells overexpressing NRBF2 was rescued when given in combination with CQ (Figure 5A). The expression of apoptosis-related cleaved PARP protein was significantly increased in SCLC cells overexpressing NRBF2 after treatment with CQ (Figure 5B). In addition, cleaved caspase 3 and TUNEL assays revealed that the reduction in apoptosis with NRBF2 overexpression in H69 and H446 cells was reversed when cells were also treated with the autophagy inhibitor CQ (Figures 5C and 5D). In accordance with the cell experiments discussed above, administering CQ restored sensitivity to chemotherapeutic drugs in an *in vivo* study, although the subcutaneous SCLC tumor model was established based on cells with NRBF2 overexpression (Figures 5E–5G). The effect of autophagy targeting treatment with endogenous expression levels of NEBF2 was identified in sensitive and resistant SCLC preclinical models.

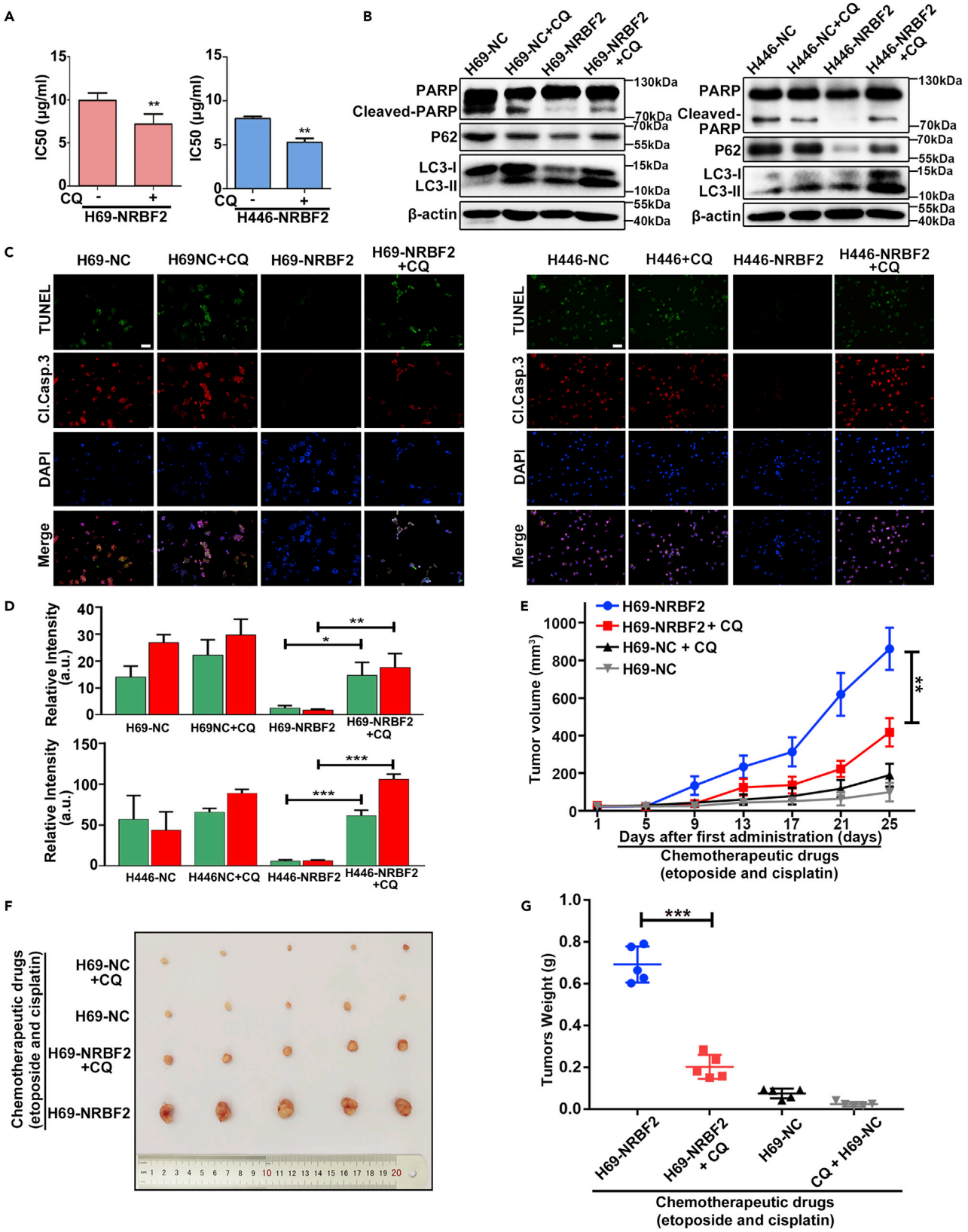
A
IC50 (μg/ml)
15
10
5
0
**
CQ - +
H69-NRBF2
IC50 (μg/ml)
15
10
5
0
**
CQ - +
H446-NRBF2
B
H69-NC
H69-NC+CQ
H69-NRBF2
H69-NRBF2 +CQ
PARP
Cleaved-PARP
P62
LC3-I
LC3-II
β-actin
130kDa
70kDa
70kDa
55kDa
15kDa
10kDa
55kDa
40kDa
H446-NC
H446-NC+CQ
H446-NRBF2
H446-NRBF2 +CQ
PARP
Cleaved-PARP
P62
LC3-I
LC3-II
β-actin
130kDa
70kDa
70kDa
55kDa
15kDa
10kDa
55kDa
40kDa
C
H69-NC
H69NC+CQ
H69-NRBF2
H69-NRBF2 +CQ
TUNEL
Cl.Casp.3
DAPI
Merge
H446-NC
H446+CQ
H446-NRBF2
H446-NRBF2 +CQ
TUNEL
Cl.Casp.3
DAPI
Merge
D
Relative Intensity (a.u.)
40
30
20
10
0
**
*
H69-NC
H69NC+CQ
H69-NRBF2
H69-NRBF2 +CQ
Relative Intensity (a.u.)
150
100
50
0
***
***
H446-NC
H446NC+CQ
H446-NRBF2
H446-NRBF2 +CQ
E
H69-NRBF2
H69-NRBF2+ CQ
H69-NC + CQ
H69-NC
Tumor volume (mm3)
1000
800
600
400
200
0
**
1
5
9
13
17
21
25
Days after first administration (days)
Chemotherapeutic drugs
(etoposide and cisplatin)
F
Chemotherapeutic drugs (etoposide and cisplatin)
H69-NC +CQ
H69-NC
H69-NRBF2 +CQ
H69-NRBF2
G
Tumors Weight (g)
1.0
0.8
0.6
0.4
0.2
0.0
***
H69-NRBF2
H69-NRBF2 + CQ
H69-NC
CQ + H69-NC
Chemotherapeutic drugs
(etoposide and cisplatin)

**Figure 5. NRBF2-induced chemoresistance is mediated by regulating autophagy**

(A) IC50 values of H69 and H444 cells with NRBF2 overexpression in the presence or absence of 10 μM CQ. **p < 0.01.

(B) Western blotting was performed to evaluate the relationship of autophagy and NRBF2 to apoptosis induced by DDP.

(C) Immunostaining for cleaved caspase 3 and TUNEL assays were performed to determine apoptosis induced by antineoplastic drugs. H69 and H446 cells stably overexpressing NRBF2 or the control in the presence or absence of 10 μM CQ. Scale bars, 50 μm.

(D) Quantification data of (C) The data are presented as the means ± SD of three independent experiments. *p < 0.05; **p < 0.01; ***p < 0.001.

(E) Tumor growth of NRBF2 overexpression or control groups was measured when treated with chemotherapy drugs (etoposide and cisplatin) alone or a combination of chemotherapy and CQ. **p < 0.01.

(F and G) Effect of chemotherapy (etoposide and cisplatin) or the combination of chemotherapy and CQ on subcutaneous tumors in nude mice. The tumor weights of different groups were measured. ***p < 0.001.

The endogenous expression of NEBF2 was not significantly different after autophagy targeting treatment of CQ (Figure S13).

Collectively, these results indicate that NRBF2-induced chemoresistance in SCLC is mediated via autophagy.

## NRBF2 directly interacts with the core autophagy protein P62

Because autophagy is a key pathway in the NRBF2-induced chemoresistance of SCLC, we must further investigate the mechanism by which NRBF2 modulates the autophagy process. To determine how NRBF2 functions in the induction of SCLC chemoresistance, a pull-down assay was conducted to identify the potential molecules interacting with NRBF2. Next, LC-MS-MS revealed potential molecules that might interact with NRBF2. Autophagic proteins from the mass spectrometry analysis were screened using the GeneCard database and published literature. Notably, P62, which is an autophagy core marker protein, was identified as a potential interactor and in the front rank of the mass spectrometry results (Figures 6A and 6B and Table S1 in supplementary material) (Ciuffa et al., 2015; Martinez-Vicente and Cuervo, 2007).

Subsequent coimmunoprecipitation (Co-IP) assays validated that NRBF2 directly interacted with P62 (Figures 6C and 6D). NRBF2 has an N-terminal microtubule-interacting and targeting (MIT) domain and a C-terminal coiled coil, together with connecting linkers (Araki et al., 2013). The domain organization of NRBF2 might elucidate protein function. Exploring how NRBF2 facilitates interactions with other cellular components will contribute to clarifying the function and related molecular mechanisms. SCLC cells were established to express MYC-tagged wild-type (WT) or mutant NRBF2 (MYC-delMIT-NRBF2 or MYC-delCoiled-coil-NRBF2) (Figure 6E). P62 protein was pulled down using an MYC antibody in cells with MYC-tagged WT NRBF2 or MYC-delCoiled-coil-NRBF2 expression, but P62 protein could not be detected in cells expressing MYC-delMIT-NRBF2 (Figure 6F). Thus, NRBF2 binds directly to the P62 protein via its MIT domain.

P62 functions as an autophagic receptor that binds to ubiquitinated cargoes and contributes to phagophore membrane formation. In the process of autophagy, P62 accumulates in ubiquitin (Ub)-positive cells, generating what is referred to as P62 bodies to provide a temporary form of storage for autophagy substrate proteins. The autophagy core protein P62 contains 3 domains that function crucially in autophagy: an N-terminal PB1 domain by which the P62 protein homopolymerizes and heterooligomerizes, a C-terminal ubiquitin-associated (UBA) domain that binds mono-Ub and poly-Ub, and an LC3-interacting (LIR) domain involved in binding to the autophagy protein LC3. ShRNA-resistant FLAG-tagged WT P62 and constructs with a deletion of the UBA, LIR, or PB1 domain (delUBA, delLIR, and delPB1) were generated for subsequent experiments (Figure 6G).

## The interaction between the MIT domain of NRBF2 and PB1 domain of P62 contributes to the formation of P62 bodies

To explore the influence of NRBF2 interacting with P62 on the process of autophagy, we identified which domains of P62 protein are necessary for NRBF2 binding. The P62 protein was stably downregulated using shRNA in SCLC cells (Figures S14A and S14B). Therafter, cells with P62 knockdown were subjected to transfection with MYC-tagged WT or mutant NRBF2 expression plasmids (MYC-delMIT-NRBF2 or MYC-delCoiled-coil-NRBF2) followed by transfection with shRNA-resistant Flag-tagged WT or mutant P62 (Flag-delUBA-P62, Flag-delLIR-P62, and Flag-delPB1-P62).

MYC antibody was applied to pull down MYC-tagged NRBF2 in the coimmunoprecipitation assay. Flag-tagged WT or mutant P62 was not coimmunoprecipitated with MYC-delMIT-NRBF2. In addition, Flag-delPB1-P62

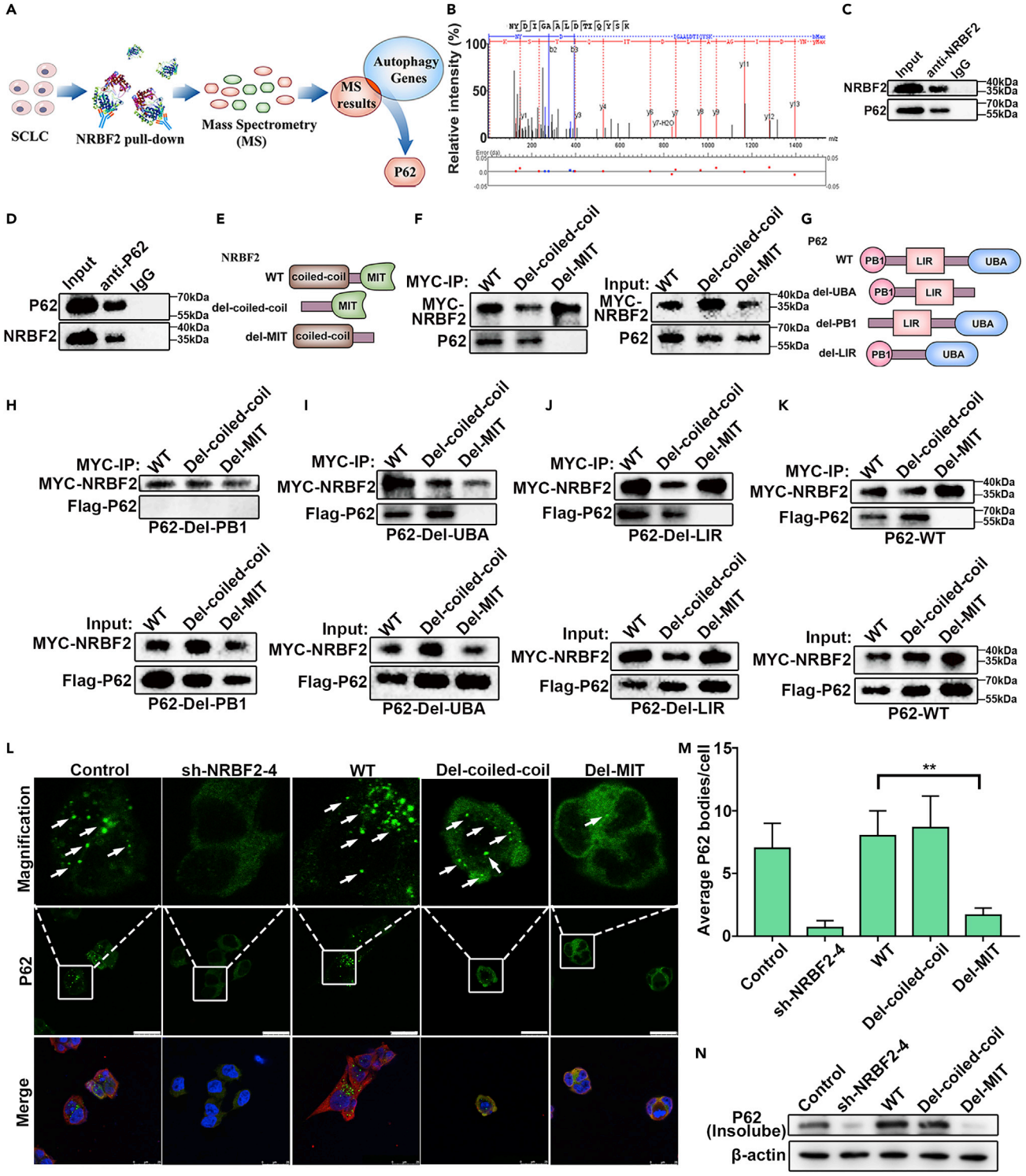


**Figure 6. The interaction between the MIT domain of NRBF2 and PB1 domain of P62 facilitates P62 body formation**

(A) Schematic diagram of screening P62 from the potential molecules interacting with NRBF2.

(B) Representative fragmentation spectrum of 421 NYDIGAALDTIQYSK 435 in the P62 protein obtained from mass spectrometry.

(C and D) Co-IP assays were conducted using specific NRBF2 and P62 antibodies in H69AR cells.

(E) Overview of NRBF2 deletion constructs used.

(F) Co-IP analysis of cells expressing MYC-tagged wild-type NRBF2 or delcoiled-coil or delMIT constructs.

**Figure 6. *Continued***

(G) Overview of the P62 wild-type and deletion constructs used.

(H–K) Co-IP assays of H69AR cells expressing MYC-tagged wild-type NRBF2 or one of its deletion construct (delMIT-NRBF2 and delCoiled-coil-NRBF2) and Flag-tagged wild-type P62 or one of its deletion constructs (Flag-delUBA-P62, Flag-delLIR-P62, and Flag-delPB1-P62).

(L) P62 bodies were analyzed by immunofluorescence assay (green: P62; red: NRBF2; blue: DAPI). Wild-type NRBF2 or one of its deletion constructs (delMIT-NRBF2 and delCoiled-coil-NRBF2) was transfected into cells with stable NRBF2 knockdown. Arrows, P62 bodies. Scale bars, 25 μm.

(M) Quantification of the average number of P62 bodies per cell from the data presented in (L). The data with standard deviations of the mean were from three independent experiments. **$p < 0.01$.

(N) Western blotting of P62 from insoluble fractions of cells transfected with wild-type NRBF2 or one of its deletion constructs (delMIT-NRBF2 and delcoiled-coil-NRBF2).

was not detected in cells expressing either MYC-tagged WT or mutant NRBF2 (Figures 6H–6K). Therefore, the MIT domain in NRBF2 interacts with the PB1 domain in P62.

The oligomerization of P62 is mediated by its N-terminal PB1 domain, resulting in target cargo recruitment into the autophagosome. Thus, we examined the effect on P62 bodies when the MIT domain of NRBF2 interacts with P62. The accumulation of P62 bodies in cells with stable NRBF2 knockdown was rescued by the transfection of WT NRBF2 or delCoiled-coil-NRBF2, whereas the transfection of delMIT-NRBF2 did not significantly increase the number of P62 bodies (Figures 6L and 6M). As aggregated proteins, including P62 bodies, are characterized by insolubility in mild detergents, such as Triton X-100, detergent-resistant extraction was performed to identify whether the NRBF2 MIT domain contributes to the formation of P62 bodies. Similarly, we found a significant reduction in the amount of P62 in the detergent-resistant fraction after transfection with delMIT-NRBF2 (Figure 6N). Deletion of the NRBF2 MIT domain abolished the formation of P62 bodies.

These results showed that the interaction of NRBF2 with P62 was necessary for architectural formation of P62 bodies, which was mediated by the NRBF2 MIT domain and P62 PB1 domain.

### NRBF2 is regulated by transcription factor XRCC6 by direct binding to the NRBF2 gene promoter

Given the important function of NRBF2 in the chemoresistance of SCLC, we further searched for the upstream regulator and unraveled the complete mechanism of NRBF2. A DNA pull-down assay was applied to identify potential interactors with the NRBF2 promoter that might control the expression of NRBF2 in SCLC chemoresistance (Figures 7A and 7B). MS analysis and screening using the Genomatix and TRRUST databases suggested that XRCC6, a transcription factor, might interact with the NRBF2 gene promoter (Figure 7C). Next, western blot analysis of the product from the DNA pull-down assay validated that the XRCC6 protein interacts with the NRBF2 gene and that the binding sites correspond to the DNA probe D sequence (Figure 7D). In a follow-up chromatin immunoprecipitation quantitative PCR (ChIP-qPCR) assay, the interaction of the transcription factor XRCC6 with the NRBF2 gene promoter was also identified. ChIP-qPCR showed markedly increased XRCC6 enrichment at the NRBF2 promoter sequence corresponding to probe D (Figure 7E). Luciferase reporter assays revealed that XRCC6 facilitated NRBF2 gene promoter transcription (Figures 7F and 7G). Notably, the differential expression of NRBF2 in chemosensitive and chemoresistant SCLC cells discussed above might be related to the differential expression of its transcription factor XRCC6, which was analyzed by western blotting (Figure 7H).

Thus, the expression of the NRBF2 gene was facilitated by the transcription factor XRCC6 by direct binding to the NRBF2 gene promoter (Figure 7I).

## DISCUSSION

Autophagy is a potential mechanism of drug resistance in tumors (Li et al., 2017; Wang et al., 2018; Zhang et al., 2015). The activation of autophagy protects tumor cells from the cytotoxic effects of chemotherapeutic drugs. However, the key molecules or detailed mechanisms associated with chemoresistance in the autophagy regulation process remain to be elucidated. In this study, we presented evidence that NRBF2 induced chemoresistance in SCLC by modulating autophagy. We showed that the drug sensitivity of SCLC cells overexpressing NRBF2 was rescued when an autophagy inhibitor was added. Targeting autophagy with CQ or hydroxychloroquine is undergoing many clinical trials in many tumors (Horne et al., 2020; Xu et al., 2018). Our studies show a significant benefit of targeting autophagy with chloroquine that could be of high clinical value and set the stage for clinical translation in SCLC chemoresistance.

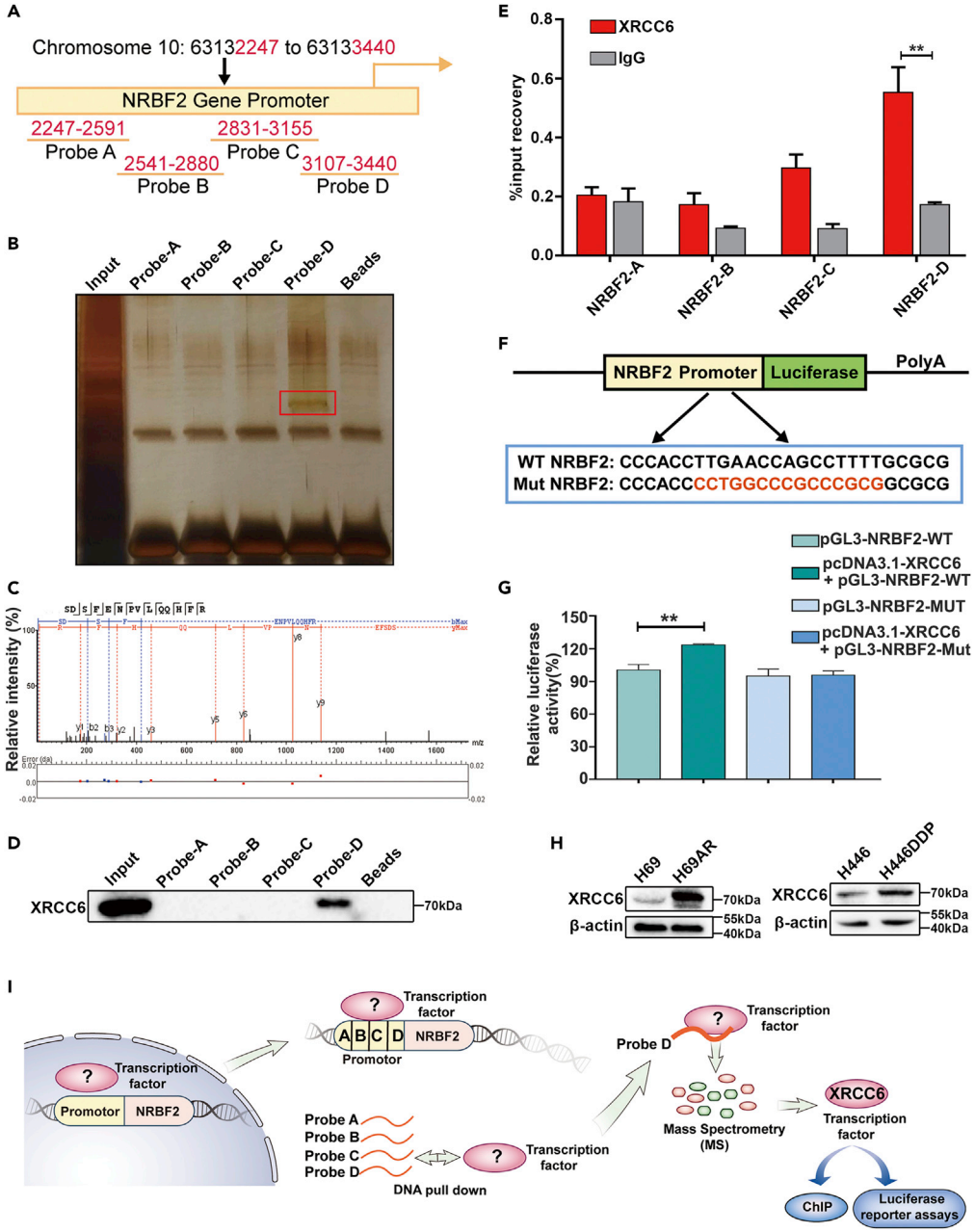


**Figure 7. The transcription factor XRCC6 regulates NRBF2 by binding to the NRBF2 gene promoter**

(A) Diagram of the NRBF2 promoter showing the locations of the different fragments tested. The fragments of the NRBF2 promoter were amplified by PCR and named DNA probes A to D. The numbers indicate the location in the NRBF2 gene promoter (chromosomes 10:63132247 to 63133440).

(B) SDS-PAGE showing proteins obtained from the DNA pulldown assay. The DNA pulldown assay was manipulated using DNA probes A to D.

(C) Representative fragmentation spectrum of 475 SDSFENPVLQQHFR 488 in XRCC6 obtained from mass spectrometry.

(D) Western blotting analysis of XRCC6 expression in the product from the DNA pulldown assay.

(E) XRCC6 ChIP-qPCR assessing XRCC6 enrichment in the regions of the NRBF2 promoter. The data are presented as means ± SD of three independent experiments. **$p < 0.01$.

(F) The luciferase reporter constructs contained wild-type (WT)-NRBF2 or mutation (Mut)-NRBF2 sequences.

(G) WT-NRBF2 or Mut-NRBF2 was cotransfected into cells with or without the pcDNA3.1-XRCC6 vector in luciferase reporter assays. The data are presented as means ± SD **$p < 0.01$.

(H) Western blotting analysis of XRCC6 expression in H69/H69AR and H446/H446DDP cells.

(I) Schematic diagram of identifying the NRBF2 gene upstream regulator.

NRBF2 is critical for the induction of autophagy and acts as a regulatory subunit of complexes required for autophagy, such as the autophagic Vps34/PIK3C3 complex (Ohashi et al., 2016). NRBF2 is involved in restricting intestinal inflammation and Alzheimer's disease by functioning as a component and regulator of the autophagy process (Wu et al., 2020; Zou et al., 2019). The function of NRBF2 has rarely been reported in the field of cancer research. A study showed that a high-risk breast cancer-related mutation site might inhibit the transcriptional activity of the NRBF2 promoter through gene enhancers, leading to a protective effect on patients (Darabi et al., 2015). However, the role of NRBF2 and NRBF2-related autophagy in tumor chemoresistance has not yet been well evaluated. It is intriguing to identify the underlying mechanism in SCLC chemoresistance. In this study, we demonstrated for the first time that NRBF2 promotes the chemoresistance of SCLC by modulating the autophagy pathway and that blocking autophagy reverses the development of chemoresistance.

The MIT domain of NRBF2 is critical for interacting with some autophagic complexes (Lu et al., 2014). Lindsey N. Young et al. found that NRBF2 induced dimerization of the autophagy-related PI3KC3-C1 complex, with implications for the higher-order organization of the preautophagosomal structure (Young et al., 2016). In this process, NRBF2 functions as the base of the PI3KC3-C1 structure, close to the ATG14L and BECN1 N termini, through its MIT domain. The function of the NRBF2 C-terminal coiled coil is also important for localization to the autophagic phagophore assembly site and homodimerization (Ohashi et al., 2016).

In this study, to further understand the biological mechanism of NRBF2 in the drug resistance of SCLC, we applied pull-down assays and LC-MS-MS to identify factors that interact with NRBF2. After screening the results from MS analysis using the GeneCard database and published literature, the autophagy receptor P62 was demonstrated to interact with the NRBF2 protein. Furthermore, deletion of the PB1 domain of P62, which regulates its homopolymerization and heterooligomerization, eliminated its interaction with NRBF2. The oligomerization of P62 is involved in the formation of P62 bodies and ubiquitin-positive and P62-positive protein bodies. P62 bodies provide a temporary form of storage for unfolded proteins to be degraded and contribute to the formation of autophagosomes (Liu et al., 2012; Szeto et al., 2006). We found that the ability of P62 to form P62 bodies was impaired by depletion of the MIT domain in NRBF2. Therefore, the mechanism by which NRBF2 induces autophagy involves the formation of P62 bodies, facilitated by the interaction between the PB1 domain of P62 and MIT domain of NRBF2.

Previous studies have shown that NRBF2 binds to ATG14L and enhances the assembly of the Atg14L-Beclin 1-Vps34-Vps15 complex for autophagy induction to prevent liver injury (Lu et al., 2014). In our study of SCLC chemoresistance, LC-MS-MS screening experiments revealed potential molecules that interact with NRBF2, but Atg14L was not identified as one of these molecules. Subsequent experiments identified the autophagy core protein P62 as the NRBF2 interactor in SCLC. The complexity and diversity of molecular biological behavior in different physiological or pathological conditions might explain why our findings were inconsistent with those of a previous study of liver injury. However, in accordance with previous studies, we found that the MIT domain of NRBF2 is indispensable for the interaction of NRBF2 with autophagic molecules and regulation of interacting protein activity for autophagy induction.

Our results suggest that the MIT domain of NRBF2 binds to the PB1 domain of P62. Previous studies have ascribed the potential functions of the PB1 domain to P62 protein oligomerization and the formation of P62 bodies (Lamark et al., 2003). In response to tumor cellular stresses such as attack from chemotherapy drugs, P62 oligomerization contributes to the formation of P62 bodies and autophagosomes. How P62 oligomerization is activated is intricate and remains to be further explored. In our study, deletion of the MIT domain of NRBF2 abolished the formation of P62 bodies in SCLC cells. This result suggests that NRBF2 is the promoter of P62 protein oligomerization in the P62-related autophagy process and that this activity occurs through interaction of the MIT domain of NRBF2 with the PB1 domain of P62. This finding accounts for the mechanism of autophagy activation in SCLC cells with NRBF2 overexpression. NRBF2 may affect the stability or flexible assembly and disassembly of the P62 scaffolds necessary for autophagosome formation mediated by its MIT domain. By identifying the behavior of NRBF2, we illuminated the potential pathomechanism of NRBF2 in the autophagy-related chemoresistance of SCLC. The association with NRBF2 expression and key lineage oncogenes such as ASCL1, NEUROD1, POU2F3, and Myc family members has not yet been reported. The key lineage oncogenes such as ASCL1, NEUROD1, POU2F3, and Myc family members were localized in the nucleus while NRBF2 in cytoplasm. ASCL1, NEUROD1, POU2F3, and Myc family members mainly functioned as transcriptional regulatory factors that play an important role in SCLC. Our study suggested that NRBF2 is a cytoplasmic autophagy regulator in the formation of autophagic P62 bodies,

leading to the chemoresistance of SCLC. The biological behavior of SCLC is a complicated course adjusted by multiple factors above. In addition, SLFN11 (schlafen family member 11) is a crucial determinant of response to DNA damaging agents, such as etoposide and cisplatin (Ballestrero et al., 2017; Berns and Berns, 2017; Murai et al., 2018; Yin et al., 2021). Once exogenous impediments stall DNA replication, SLFN11 immediately irreversibly blocks replication via activation of the DNA damage response network and induction of cell-cycle arrest (Murai et al., 2019). Autophagy is another stress response for cellular homeostasis to disassemble unnecessary or dysfunctional cellular components and accumulating research works suggest that autophagy promotes resistance to chemotherapy. In our study, NRBF2 promotes the autophagy process through facilitating the formation of P62 bodies in response to cellular stresses from chemotherapy. We speculate that the balance of SLFN11-related response and NRBF2-related autophagy might be a crucial cell fate determinant under the treatment of chemotherapy drugs. However, the relationship of SLFN11 expression and NRBF2-related autophagy has yet to be fully understood and needs to be further explored. In our study, the regulation of SLFN11 could not significantly affect autophagy and the NRBF2 expression in SCLC cells, thus SLFN11 and NRBF2 may function by different mechanisms.

Notably, our findings revealed that the transcription factor XRCC6 protein directly regulates the NRBF2 gene promoter, resulting in the differential expression of NRBF2 in chemosensitive and chemoresistant SCLC. XRCC6 plays an important role in DNA recombination and repair to support genome stability, and it is crucial for fundamental cellular processes, such as metabolism and aging, and related diseases, such as cancers (Kim et al., 2012; Rathaus et al., 2009; Wang et al., 2013). The association of XRCC6 and the risk of lung cancer have been established in several experiments (Hsia et al., 2012; Jia et al., 2015; Zhu et al., 2016). We revealed the biological function of XRCC6 in NRBF2-induced chemoresistance for the first time. XRCC6 targeting may be a therapeutic strategy that can be combined with NRBF2 targeting for patients with drug-resistant SCLC.

Taken together, our results demonstrated that NRBF2 promotes the chemoresistance of SCLC by inducing autophagy. Furthermore, we identified that the interaction between the MIT domain of NRBF2 and PB1 domain of P62 contributes to the formation of autophagic P62 bodies in the NRBF2-related autophagy process, leading to the chemoresistance of SCLC. Thus, NRBF2 is likely a useful marker for chemotherapy response in SCLC. According to the identified effects of NRBF2 on autophagy, targeting NRBF2 likely inhibits autophagy and is a potential therapeutic approach for drug-resistant SCLC.

### Limitations of the study

Although we showed that NRBF2 promotes the chemoresistance of SCLC by inducing autophagy, substrates of NRBF2-related autophagic degradation and how they function on chemoresistance need to be further explored.

## STAR★METHODS

Detailed methods are provided in the online version of this paper and include the following:

- KEY RESOURCES TABLE
- RESOURCE AVAILABILITY
  - Lead contact
  - Materials availability
  - Data and code availability
- EXPERIMENTAL MODEL AND SUBJECT DETAILS
  - Cell lines
  - Tumor specimens
  - SCLC cell line-derived tumor xenografts
  - Patient-derived tumor xenograft (PDX) establishment
  - Generation of chemoresistant subcutaneous PDX model
  - Ethics committee approval
- METHOD DETAILS
  - RNA extractions, sequencing and data processing
  - Cell counting kit-8 (CCK-8) assays and IC50 calculation
  - Western blot analysis
  - Transmission electron microscopy (TEM)

- Cell apoptosis assay
- Immunohistochemistry (IHC)
- mRFP-GFP-LC3 adenovirus translocation and analysis
- Lentivirus production and plasmids used
- Co-immunoprecipitation (Co-IP)
- Mass spectrometry (MS)
- Chromatin immunoprecipitation quantitative PCR (ChIP-qPCR) assay
- Pull-down assay
- Construction of plasmids and luciferase reporter assays

● QUANTIFICATION AND STATISTICAL ANALYSIS

## SUPPLEMENTAL INFORMATION

Supplemental information can be found online at https://doi.org/10.1016/j.isci.2022.104471.

## ACKNOWLEDGMENTS

This work was supported by grants from the National Science Foundation of China (81772457, 81802257, 81802254, 82172750, and 81871859), China Postdoctoral Science Foundation funded project (2020M682813), the Science and Technology Planning Project of Guangdong Province (Grant No. 2019A030317020), Guangzhou Science and Technology Project (201804010200), and Province Natural Science Foundation of Guangdong (2018A030313846). We thank Ge Wen from Guangzhou Bioillus Co. Ltd. for his assistance in editing the schematic diagram.

## AUTHOR CONTRIBUTIONS

T.W., J.Z., and W.S. designed the study. W.S., P.L., W. Z., N.Z., Q.W., and Y.S. performed the experiments. H.Z., Q.Z., A. L., Q.C., and J.S. analyzed the experimental data. W.S. and Q.Z. wrote the manuscript. T.W., J.Z., and H.W. revised the manuscript.

## DECLARATION OF INTERESTS

The authors declare no competing interests.

Received: November 4, 2021
Revised: February 22, 2022
Accepted: May 20, 2022
Published: June 17, 2022

## REFERENCES

Araki, Y., Ku, W.C., Akioka, M., May, A.I., Hayashi, Y., Arisaka, F., Ishihama, Y., and Ohsumi, Y. (2013). Atg38 is required for autophagy-specific phosphatidylinositol 3-kinase complex integrity. J. Cell Biol. *203*, 299–313. https://doi.org/10.1083/jcb.201304123.

Ballestrero, A., Bedognetti, D., Ferraioli, D., Franceschelli, P., Labidi-Galy, S.I., Leo, E., Murai, J., Pommier, Y., Tsantoulis, P., Vellone, V.G., and Zoppoli, G. (2017). Report on the first SLFN11 monothematic workshop: from function to role as a biomarker in cancer. J. Transl. Med. *15*, 199. https://doi.org/10.1186/s12967-017-1296-3.

Berns, K., and Berns, A. (2017). Awakening of "Schlafen11" to tackle chemotherapy resistance in SCLC. Cancer Cell *31*, 169–171. https://doi.org/10.1016/j.ccell.2017.01.013.

Ciuffa, R., Lamark, T., Tarafder, A.K., Guesdon, A., Rybina, S., Hagen, W.J., Johansen, T., and Sachse, C. (2015). The selective autophagy receptor p62 forms a flexible filamentous helical scaffold. Cell Rep. *11*, 748–758. https://doi.org/10.1016/j.celrep.2015.03.062.

Darabi, H., McCue, K., Beesley, J., Michailidou, K., Nord, S., Kar, S., Humphreys, K., Thompson, D., Ghoussaini, M., Bolla, M.K., et al. (2015). Polymorphisms in a putative enhancer at the 10q21.2 breast cancer risk locus regulate NRBF2 expression. Am. J. Hum. Genet. *97*, 22–34. https://doi.org/10.1016/j.ajhg.2015.05.002.

Hamilton, G., Hochmair, M., Rath, B., Klameth, L., and Zeillinger, R. (2016). Small cell lung cancer: circulating tumor cells of extended stage patients express a mesenchymal-epithelial transition phenotype. Cell Adhes. Migrat. *10*, 360–367. https://doi.org/10.1080/19336918.2016.1155019.

Horne, G.A., Stobo, J., Kelly, C., Mukhopadhyay, A., Latif, A.L., Dixon-Hughes, J., McMahon, L., Cony-Makhoul, P., Byrne, J., Smith, G., et al. (2020). A randomised phase II trial of hydroxychloroquine and imatinib versus imatinib alone for patients with chronic myeloid leukaemia in major cytogenetic response with residual disease. Leukemia *34*, 1775–1786. https://doi.org/10.1038/s41375-019-0700-9.

Hsia, T.C., Liu, C.J., Chu, C.C., Hang, L.W., Chang, W.S., Tsai, C.W., Wu, C.I., Lien, C.S., Liao, W.L., Ho, C.Y., and Bau, D.T. (2012). Association of DNA double-strand break gene XRCC6 genotypes and lung cancer in Taiwan. Anticancer Res. *32*, 1015–1020.

Jacob, J.A., Salmani, J.M.M., Jiang, Z., Feng, L., Song, J., Jia, X., and Chen, B. (2017). Autophagy: an overview and its roles in cancer and obesity. Clin. Chim. Acta *468*, 85–89. https://doi.org/10.1016/j.cca.2017.01.028.

Janku, F., McConkey, D.J., Hong, D.S., and Kurzrock, R. (2011). Autophagy as a target for anticancer therapy. Nat. Rev. Clin. Oncol. *8*, 528–539. https://doi.org/10.1038/nrclinonc.2011.71.

Jia, J., Ren, J., Yan, D., Xiao, L., and Sun, R. (2015). Association between the XRCC6 polymorphisms and cancer risks: a systematic review and meta-analysis. Medicine *94*, e283. https://doi.org/10.1097/md.0000000000000283.

Kim, M., Jung, J.Y., Choi, S., Lee, H., Morales, L.D., Koh, J.T., Kim, S.H., Choi, Y.D., Choi, C., Slaga, T.J., et al. (2017). GFRA1 promotes cisplatin-induced chemoresistance in osteosarcoma by inducing autophagy. Autophagy *13*, 149–168. https://doi.org/10.1080/15548627.2016.1239676.

Kim, S., Bi, X., Czarny-Ratajczak, M., Dai, J., Welsh, D.A., Myers, L., Welsch, M.A., Cherry, K.E., Arnold, J., Poon, L.W., and Jazwinski, S.M. (2012). Telomere maintenance genes SIRT1 and XRCC6 impact age-related decline in telomere length but only SIRT1 is associated with human longevity. Biogerontology *13*, 119–131. https://doi.org/10.1007/s10522-011-9360-5.

Lamark, T., Perander, M., Outzen, H., Kristiansen, K., Øvervatn, A., Michaelsen, E., Bjørkøy, G., and Johansen, T. (2003). Interaction codes within the family of mammalian Phox and Bem1p domain-containing proteins. J. Biol. Chem. *278*, 34568–34581. https://doi.org/10.1074/jbc.m303221200.

Lawson, M.H., Cummings, N.M., Rassl, D.M., Russell, R., Brenton, J.D., Rintoul, R.C., and Murphy, G. (2011). Two novel determinants of etoposide resistance in small cell lung cancer. Cancer Res. *71*, 4877–4887. https://doi.org/10.1158/0008-5472.can-11-0080.

Li, Y.J., Lei, Y.H., Yao, N., Wang, C.R., Hu, N., Ye, W.C., Zhang, D.M., and Chen, Z.S. (2017). Autophagy and multidrug resistance in cancer. Chin. J. Cancer *36*, 52. https://doi.org/10.1186/s40880-017-0219-2.

Liu, X.D., Ko, S., Xu, Y., Fattah, E.A., Xiang, Q., Jagannath, C., Ishii, T., Komatsu, M., and Eissa, N.T. (2012). Transient aggregation of ubiquitinated proteins is a cytosolic unfolded protein response to inflammation and endoplasmic reticulum stress. J. Biol. Chem. *287*, 19687–19698. https://doi.org/10.1074/jbc.m112.350934.

Lu, J., He, L., Behrends, C., Araki, M., Araki, K., Jun Wang, Q., Catanzaro, J.M., Friedman, S.L., Zong, W.X., Fiel, M.I., et al. (2014). NRBF2 regulates autophagy and prevents liver injury by modulating Atg14L-linked phosphatidylinositol-3 kinase III activity. Nat. Commun. *5*, 3920. https://doi.org/10.1038/ncomms4920.

Martinez-Vicente, M., and Cuervo, A.M. (2007). Autophagy and neurodegeneration: when the cleaning crew goes on strike. Lancet Neurol. *6*, 352–361. https://doi.org/10.1016/s1474-4422(07)70076-5.

Murai, J., Tang, S.W., Leo, E., Baechler, S.A., Redon, C.E., Zhang, H., Al Abo, M., Rajapakse, V.N., Nakamura, E., Jenkins, L.M.M., et al. (2018). SLFN11 blocks stressed replication forks independently of ATR. Mol. Cell *69*, 371–384.e6. https://doi.org/10.1016/j.molcel.2018.01.012.

Murai, J., Thomas, A., Miettinen, M., and Pommier, Y. (2019). Schlafen 11 (SLFN11), a restriction factor for replicative stress induced by DNA-targeting anti-cancer therapies. Pharmacol. Ther. *201*, 94–102. https://doi.org/10.1016/j.pharmthera.2019.05.009.

Ohashi, Y., Soler, N., García Ortegón, M., Zhang, L., Kirsten, M.L., Perisic, O., Masson, G.R., Burke, J.E., Jakobi, A.J., Apostolakis, A.A., et al. (2016). Characterization of Atg38 and NRBF2, a fifth subunit of the autophagic Vps34/PIK3C3 complex. Autophagy *12*, 2129–2144. https://doi.org/10.1080/15548627.2016.1226736.

Rathaus, M., Lerrer, B., and Cohen, H.Y. (2009). DeubiKuitylation: a novel DUB enzymatic activity for the DNA repair protein, Ku70. Cell Cycle *8*, 1843–1852. https://doi.org/10.4161/cc.8.12.8864.

Rubinsztein, D.C., Codogno, P., and Levine, B. (2012). Autophagy modulation as a potential therapeutic target for diverse diseases. Nat. Rev. Drug Discov. *11*, 709–730. https://doi.org/10.1038/nrd3802.

Rudin, C.M., and Poirier, J.T. (2017). Shining light on novel targets and therapies. Nat. Rev. Clin. Oncol. *14*, 75–76. https://doi.org/10.1038/nrclinonc.2016.203.

Sabari, J.K., Lok, B.H., Laird, J.H., Poirier, J.T., and Rudin, C.M. (2017). Unravelling the biology of SCLC: implications for therapy. Nat. Rev. Clin. Oncol. *14*, 549–561. https://doi.org/10.1038/nrclinonc.2017.71.

Shen, W., Zhang, W., Ye, W., Wang, H., Zhang, Q., Shen, J., Hong, Q., Li, X., Wen, G., Wei, T., and Zhang, J. (2020). SR9009 induces a REV-ERB dependent anti-small-cell lung cancer effect through inhibition of autophagy. Theranostics *10*, 4466–4480. https://doi.org/10.7150/thno.42478.

Shen, W., Zhang, X., Fu, X., Fan, J., Luan, J., Cao, Z., Yang, P., Xu, Z., and Ju, D. (2017). A novel and promising therapeutic approach for NSCLC: recombinant human arginase alone or combined with autophagy inhibitor. Cell Death Dis. *8*, e2720. https://doi.org/10.1038/cddis.2017.137.

Siegel, R.L., Miller, K.D., Fedewa, S.A., Ahnen, D.J., Meester, R.G.S., and Barzi, A. (2017). Colorectal cancer statistics, 2017. CA Cancer J. Clin. *67*, 177–193. https://doi.org/10.3322/caac.21395.

Sun, W.L., Chen, J., Wang, Y.P., and Zheng, H. (2011). Autophagy protects breast cancer cells from epirubicin-induced apoptosis and facilitates epirubicin-resistance development. Autophagy *7*, 1035–1044. https://doi.org/10.4161/auto.7.9.16521.

Szeto, J., Kaniuk, N.A., Canadien, V., Nisman, R., Mizushima, N., Yoshimori, T., Bazett-Jones, D.P., and Brumell, J.H. (2006). ALIS are stress-induced protein storage compartments for substrates of the proteasome and autophagy. Autophagy *2*, 189–199. https://doi.org/10.4161/auto.2731.

Wang, Q., Zeng, F., Sun, Y., Qiu, Q., Zhang, J., Huang, W., Huang, J., Huang, X., and Guo, L. (2018). Etk interaction with PFKFB4 modulates chemoresistance of small-cell lung cancer by regulating autophagy. Clin. Cancer Res. *24*, 950–962. https://doi.org/10.1158/1078-0432.ccr-17-1475.

Wang, Z., Lin, H., Hua, F., and Hu, Z.W. (2013). Repairing DNA damage by XRCC6/KU70 reverses TLR4-deficiency-worsened HCC development via restoring senescence and autophagic flux. Autophagy *9*, 925–927. https://doi.org/10.4161/auto.24229.

Wu, M.Y., Liu, L., Wang, E.J., Xiao, H.T., Cai, C.Z., Wang, J., Su, H., Wang, Y., Tan, J., Zhang, Z., et al. (2020). PI3KC3 complex subunit NRBF2 is required for apoptotic cell clearance to restrict intestinal inflammation. Autophagy *17*, 1096–1111. https://doi.org/10.1080/15548627.2020.1741332.

Xu, R., Ji, Z., Xu, C., and Zhu, J. (2018). The clinical value of using chloroquine or hydroxychloroquine as autophagy inhibitors in the treatment of cancers: a systematic review and meta-analysis. Medicine *97*, e12912. https://doi.org/10.1097/md.0000000000012912.

Yin, Y.P., Ma, L.Y., Cao, G.Z., Hua, J.H., Lv, X.T., and Lin, W.C. (2021). FK228 potentiates topotecan activity against small cell lung cancer cells via induction of SLFN11. Acta Pharmacol. Sin. https://doi.org/10.1038/s41401-021-00817-y.

Young, L.N., Cho, K., Lawrence, R., Zoncu, R., and Hurley, J.H. (2016). Dynamics and architecture of the NRBF2-containing phosphatidylinositol 3-kinase complex I of autophagy. Proc. Natl. Acad. Sci. U S A *113*, 8224–8229. https://doi.org/10.1073/pnas.1603650113.

Zhang, S.F., Wang, X.Y., Fu, Z.Q., Peng, Q.H., Zhang, J.Y., Ye, F., Fu, Y.F., Zhou, C.Y., Lu, W.G., Cheng, X.D., and Xie, X. (2015). TXNDC17 promotes paclitaxel resistance via inducing autophagy in ovarian cancer. Autophagy *11*, 225–238. https://doi.org/10.1080/15548627.2014.998931.

Zhu, B., Cheng, D., Li, S., Zhou, S., and Yang, Q. (2016). High expression of XRCC6 promotes human osteosarcoma cell proliferation through the β-catenin/Wnt signaling pathway and is associated with poor prognosis. Int. J. Mol. Sci. *17*, 1188. https://doi.org/10.3390/ijms17071188.

Zou, D., Li, R., Huang, X., Chen, G., Liu, Y., Meng, Y., Wang, Y., Wu, Y., and Mao, Y. (2019). Identification of molecular correlations of RBM8A with autophagy in Alzheimer's disease. Aging *11*, 11673–11685. https://doi.org/10.18632/aging.102571.

## STAR★METHODS

### KEY RESOURCES TABLE

| REAGENT or RESOURCE | SOURCE | IDENTIFIER |
|---|---|---|
| Antibodies | | |
| NRBF2 | Proteintech Group | Cat#: 24858-1-AP; RRID: AB_2879759 |
| MYC | Proteintech Group | Cat#: 16286-1-AP; RRID: AB_11182162 |
| Flag | Proteintech Group | Cat#: 20543-1-AP; RRID: AB_11232216 |
| XRCC6 | Proteintech Group | Cat#: 10723-1-AP; RRID: AB_2218756 |
| β-actin | Cell Signaling Technology | Cat#: 4970; RRID: AB_2223172 |
| LC3B | Cell Signaling Technology | Cat#: 83506; RRID: AB_2800018 |
| SQSTM1/p62 | Cell Signaling Technology | Cat#: 88588; RRID: AB_2800125 |
| cleaved caspase 3 | Cell Signaling Technology | Cat#: 9661; RRID: AB_2341188 |
| PARP | Cell Signaling Technology | Cat#: 9532; RRID: AB_659884 |
| Goat Anti-Rabbit IgG antibody (HRP) | Abcam | Cat#: ab205718; RRID: AB_2819160 |
| Goat Anti-Mouse IgG antibody (HRP) | Abcam | Cat#: ab97240; RRID: AB_10695944 |
| Chemicals, peptides, and recombinant proteins | | |
| PBS | Gibco | Cat#: 70011-044 |
| Penicillin-streptomycin solution | Solarbio | Cat#: P1400 |
| RIPA | Beyotime | Cat#: P0013 |
| Skim milk | BD | Cat#: BD-232100 |
| Experimental models: Cell lines | | |
| Human:H69AR | ATCC | Cat#: CRL-11351 |
| Human:H69 | ATCC | Cat#: HTB-119 |
| Human:H446 | ATCC | Cat#: HTB-171 |
| Experimental models: Organisms/strains | | |
| Mouse: BALB/c nude mice | Experimental Animal Center of Southern Medical University | N/A |
| Mouse: NCG mice | GemPharmatech | N/A |
| Software and algorithms | | |
| GraphPad Prism Software | GraphPad | https://www.graphpad.com |

### RESOURCE AVAILABILITY

#### Lead contact

Further information and requests for resources and reagents should be directed to and will be fulfilled by the lead contact, Ting Wei (weitingyouyou@qq.com).

#### Materials availability

This study did not generate new unique reagents.

#### Data and code availability

All data reported in this paper will be shared by the Lead contact upon request.

This paper does not report original code.

Any additional information required to reanalyze the data reported in this paper is available from the Lead contact upon request.

## EXPERIMENTAL MODEL AND SUBJECT DETAILS

### Cell lines

Human SCLC cell lines NCI-H69 and NCI-H446 and chemoresistant H69AR cells were purchased from American Type Culture Collection (ATCC). The other chemoresistant subline, H446DDP, was established in our laboratory by culturing H446 cells in cisplatin. The drug-resistant H446DDP cell line was cultured in gradually increasing concentraion of cisplatin up to 2.0 μM after a total of 7 months. H69AR and H446DDP were maintained in drug-free medium for at least 2 weeks before any experiment. Cells were grown at 37°C and 5% $CO_2$ in RPMI 1640 medium supplemented with 10% foetal bovine serum and 1% penicillin-streptomycin solution.

### Tumor specimens

45 SCLC samples was collected from Zhujiang Hospital of Southern Medical University and Sun Yat-Sen University Cancer Center. Data including gender, age, smoking status, stage was showed in Table S2 in supplementary material. This study was approved by the Ethics Committee of Zhujiang Hospital of Southern Medical University and Sun Yat-Sen University Cancer Center, and all patients provided informed consent.

### SCLC cell line-derived tumor xenografts

Female BALB/c nude mice were obtained from the Experimental Animal Center of Southern Medical University (Guangzhou, China) and maintained under specific pathogen-free conditions. Cells were collected and suspended in culture medium. In total, $1 \times 10^7$ cells stably transfected with NRBF2/shNRBF2 or the corresponding control lentiviral particles were subcutaneously injected into the mice to establish the SCLC xenograft model. The mice were intraperitoneally injected with saline containing chemotherapeutics or saline alone as a control. The mice received intraperitoneal injections of etoposide (4 mg/kg) once every 2 days and cisplatin (2 mg/kg) once every 8 days. The tumor sizes were measured and calculated using the following ellipsoid volume formula: V = (length × width 2/2).

### Patient-derived tumor xenograft (PDX) establishment

Primary SCLC tissue samples for PDX model establishment were anonymized and obtained from Zhujiang Hospital of Southern Medical University (Guangzhou, China). SCLC tumor samples were minced with surgical scissors into fragments (approximately 3 $mm^3$) and implanted subcutaneously into the flanks of severely immunodeficient female NCG mice (GemPharmatech, Nanjing, China). The animals were observed daily to assess tumor growth. When the tumor size exceeded approximately 1500 $mm^3$, the animals were euthanized, and the xenografts were removed. Subsequently, xenograft fragments were implanted into new mice for passaging.

### Generation of chemoresistant subcutaneous PDX model

The PDX model established above was treated with cisplatin (2.5 mg/kg, i.p. injection on day 1) and etoposide (4 mg/kg, i.p. injection on days 1–3) once every ten days. The mice were euthanized, and the tumors were removed as the tumor volume reached approximately 500 $mm^3$. Tumor xenografts were cut into small fragments and serially passaged using the same technique until chemoresistant tumors developed.

### Ethics committee approval

This study was approved by the Ethics Committee of Zhujiang Hospital of Southern Medical University and Sun Yat-Sen University Cancer Center. Informed consent in studies involving human tissue was obtained from all the patients before specimen collection. All the animal experiments were performed with the approval of the Ethics Committee for Animal Experimentation of the Zhujiang Hospital of Southern Medical University.

## METHOD DETAILS

### RNA extractions, sequencing and data processing

For RNA extractions, tissue sections were first lysed and homogenized with the TissueLyser (Qiagen). Subsequent RNA extractions were performed with the Qiagen RNeasy Mini Kit according to the instructions provided by the manufacturer. The RNA quality was assessed with a Bioanalyzer 2100 DNA Chip 7500 (Agilent Technologies), and samples with an RNA integrity number (RIN) of over 7 were further analyzed by

RNA-seq. All sequencing reactions were performed on an Illumina HiSeq 2000 instrument (Illumina, San Diego, CA, USA). RNA-seq was performed with RNA extracted from FFPE samples (n = 45). cDNA libraries were prepared from poly(A)-selected RNA by applying the Illumina TruSeq protocol for mRNA. The libraries were then sequenced with a 2 × 100 bp paired-end protocol. We used HISAT2 (version 2.1.0) with the default setting to map the RNA-seq data to the human reference genome (NCBI38/hg38). We aggregated the read counts at the gene level using HTSeq.

### Cell counting kit-8 (CCK-8) assays and IC50 calculation

Drug resistance and cell viability were measured using the Cell Count Kit-8 assay (CCK-8, Dojindo, Kumamoto, Japan). The SCLC cells were seeded at 5000 cells per well in 96-well plates and subjected to different doses of chemotherapeutic drugs. Cell viability was measured after incubation with the drugs for 24 h at 37°C using a CCK-8 assay. Absorbance was detected at 450 nm after treatment with 10 μL of CCK-8 reagent. The results were normalized to the control. The IC50 values were calculated using GraphPad Prism software, and the comparison of IC50 values between different groups was performed by unpaired t-tests.

### Western blot analysis

Cells were collected and washed with cold PBS and then incubated at 0°C for 30 min in cell lysis buffer. The soluble and insoluble fractions of proteins were extracted. The protein concentration was examined using the bicinchoninic acid method. Equal quantities of protein were separated by polyacrylamide gel electrophoresis and subsequently transferred to PVDF membranes. The membranes were blocked with 5% bovine serum albumin in Tris-buffered saline with Tween 20 (TBST). After that, the PVDF membranes were incubated at 4°C in the corresponding primary antibody overnight, and then the membranes were washed three times each for at least 15 min. After washing, the membranes were incubated in secondary horseradish peroxidase-conjugated antibody for 1.5 h. Finally, signals were detected using enhanced chemiluminescence reagents.

### Transmission electron microscopy (TEM)

2.5% glutaraldehyde containing 0.1 mol/L sodium cacodylate was used to fixed with SCLC cells and cells were treated with 1% osmium tetroxide. Then samples were embedded in araldite, cut into thin sections, and stained with uranyl acetate and lead citrate. A JEM 1400 transmission electron microscope (JEOL, Inc., Peabody, MA, USA) at 80 kV was applied to examined the autophagic vesicles.

### Cell apoptosis assay

Immunostaining for cleaved caspase 3 was performed to evaluate cell apoptosis, and the TUNEL assay was performed using an *In Situ* Cell Death Detection Kit, Fluorescein (Roche) according to the manufacturer's protocol. Cell apoptosis was analyzed with a fluorescence microscope equipped with a digital camera.

### Immunohistochemistry (IHC)

Tissue samples of the subcutaneous SCLC tumor models were fixed in 4% paraformaldehyde and then embedded in paraffin blocks. Four-micron-thick sections were cut and analyzed for NRBF2 and P62 protein expression. The slides were incubated first with anti-NRBF2 or anti-P62 antibodies at 4°C overnight and then with secondary antibodies for 2 h. The results were evaluated using the EnVision peroxidase system (Dako).

### mRFP-GFP-LC3 adenovirus translocation and analysis

The mRFP-GFP-LC3 adenovirus was applied to label and track autophagy marker LC3. The weakening of GFP can indicate the fusion of lysosomes and autophagosomes to form autolysosomes because GFP fluorescent protein is sensitive to acidity. After the fusion of the lysosomes and the autophagosomes, the GFP fluorescence is quenched, and only red fluorescence can be detected at this time. This tandem fluorescent protein expression vector system intuitively and clearly indicates the level of autophagic flux. SCLC cells were seeded in glass-bottomed cell culture dishes (NEST Biotechnology Co., LTD.) at a density of $1 \times 10^3$ cells/mL. When the SCLC cells reached approximately 30% confluence, they were transfected with the mRFP-GFP-LC3 adenovirus for 6 h. Next, the medium was removed and washed twice with PBS. The cells were incubated for 48h at 37°C and 5% $CO_2$ in serum-containing RPMI 1640 medium. After incubation, the cells were washed twice with PBS. Image acquisition was performed using a laser scanning confocal microscope (LSM880, Carl Zeiss, Germany).

### Lentivirus production and plasmids used

Cells were transfected with the lentiviral particles of shNRBF2, NRBF2 or shP62 (Genecopoeia, Inc., Rockville, MD, USA). The Flag-WT-P62, Flag-delUBA-P62, Flag-delLIR-P62, and Flag-delPB1-P62 constructs were purchased from Genecopoeia, Inc. MYC-WT-NRBF2, MYC-delMIT-NRBF2 and MYC-delCoiled-coil-NRBF2 were also purchased from Genecopoeia, Inc. The transfection process was performed using lipofectamine 2000 following the manufacturer's instructions. Virus particles were harvested 2 days after transfection. Cells were infected in the presence of Opti-MEM medium supplemented with polybrene.

### Co-immunoprecipitation (Co-IP)

The cell protein lysate was incubated overnight at 4°C together with antibodies. Next, preblocked agarose beads were added to the mixture and incubated for 2 h at 4°C. The mixture was washed three times with 1 mL of lysis buffer and eluted from the beads for western blot analysis. Proteins were detected using the anti-NRBF2, anti-P62, anti-MYC or anti-Flag antibody.

### Mass spectrometry (MS)

The immunoprecipitated protein was detected using liquid chromatography-tandem mass spectrometry (LC-MS-MS), and accurate high-resolution mass data were obtained using a Q Exactive Orbitrap mass spectrometer (Thermo Scientific).

### Chromatin immunoprecipitation quantitative PCR (ChIP-qPCR) assay

Chromatin immunoprecipitation was performed using the Magna ChIP™ A/G Chromatin Immunoprecipitation Kit with an antibody specific for XRCC6 or normal rabbit IgG. Following chromatin immunoprecipitation, immunoprecipitated DNA extracted from SCLC cells was analyzed by qPCR using specific primers.

### Pull-down assay

The promoter region of the NRBF2 gene was amplified by PCR using biotin-labelled dCTP. The 5′-biotinylated DNA of the 5′-flanking regions of the NRBF2 gene was immobilized on streptavidin beads. Proteins in the nuclear fraction were incubated with 5′-biotinylated DNA beads at 4°C overnight. Afterwards, the supernatant was removed. The beads were washed three times with cold PBS. The mixture was then resuspended in distilled water at 70°C for 3 min to break the bond between streptavidin and biotin. The eluted proteins from the beads without the biotinylated DNA probe were used as controls. Each group of proteins was separated by polyacrylamide gel electrophoresis. Silver nitrate staining and MS analyses were then performed and detected using liquid chromatography-tandem mass spectrometry, and accurate high-resolution mass data were obtained using a Q Exactive Orbitrap mass spectrometer (Thermo Scientific).

### Construction of plasmids and luciferase reporter assays

To generate the pcDNA3.1-XRCC6 plasmid, we amplified and cloned the XRCC6 coding sequence (CDS) into the pcDNA3.1 vector (Promega, CA, USA) using the Nhe1 and Not1 restriction enzymes. The NRBF2 promoter sequences, including NRBF2-WT and NRBF2-MUT, were amplified and cloned into the pGL3 vector with the firefly luciferase gene by the Nhe1 and Xho1 restriction enzymes. SCLC cells were cotransfected with pcDNA3.1-XRCC6, pGL3-NRBF2-WT, pGL3-NRBF2-MUT and control plasmids using Lipofectamine 2000 following the manufacturer's instructions. Subsequently, the luciferase activity was measured using a dual reporter luciferase assay kit (Promega, USA). The relative luciferase activity of the target promoter was represented by firefly luciferase activity, which was normalized to Renilla luciferase activity. Three individual transfection experiments were performed.

## QUANTIFICATION AND STATISTICAL ANALYSIS

The data in this study were analyzed using GraphPad Prism Software (GraphPad Software, Inc., La Jolla, CA, USA). The data were presented as means ± SD Student's t-test or one-way ANOVA was applied for comparisons between two groups. Differences with p-values $< 0.05$ were considered statistically significant. $p < 0.05$, $<0.01$ and $<0.001$ are indicated as *, ** and ***, respectively.